



## Novel hydrogen gas sensor based on single ZnO nanorod

Oleg Lupan<sup>a,b,\*</sup>, Guangyu Chai<sup>c</sup>, Lee Chow<sup>a</sup>

<sup>a</sup> Department of Physics, University of Central Florida, 4000 Central Florida Boulevard, Orlando, FL 32816-2385, USA

<sup>b</sup> Department of Microelectronics and Semiconductor Devices, Technical University of Moldova, 168 Stefan cel Mare Boulevard, Chisinau MD-2004, Republic of Moldova

<sup>c</sup> Apollo Technologies Inc., 205 Waymont Court, S111, Lake Mary, FL 32746, USA

### ARTICLE INFO

#### Article history:

Received 3 March 2008

Received in revised form 26 June 2008

Accepted 27 June 2008

Available online 17 July 2008

#### PACS:

81.07.-b

87.07.Df

81.16.Be

#### Keywords:

Nanofabrication

Nanoscale materials and structures

Gas sensor

Hydrogen

ZnO nanorod

### ABSTRACT

For extensive use in an industrialized process of individual ZnO nano/microrods as building nanoblock in novel hydrogen sensors, a simple, inexpensive, and bio-safe synthesis process and nanofabrication route is required. Here, we report a cost-effective and fast synthesis route for ZnO one-dimensional nanorod using an aqueous-based approach in a reactor. Our synthesis technique permits nano/microrods to be easily transferred to other substrates and to be distributed on the surface. This flexibility of substrate choice opens the possibility of using focused ion beam (FIB/SEM) system for handling and fabricating nanosensors. The main advantage of this procedure is a quick verification/testing of concept and is compatible with micro/nanoelectronic devices. The described nanofabrication steps permitted us to obtain a 90% success rate for building single nanorod sensor. A sensitivity of  $\sim 4\%$  was obtained for a single ZnO nanorod hydrogen sensor at 200 ppm H<sub>2</sub> in the air at room temperature. The nanosensor has a high selectivity for H<sub>2</sub>, since its sensitivity for O<sub>2</sub>, CH<sub>4</sub>, CO, ethanol or LPG are less than 0.25%.

© 2008 Elsevier B.V. All rights reserved.

### 1. Introduction

Hydrogen (H<sub>2</sub>) is expected to supplant hydrocarbons and becomes “the common fuel of the future” [1]. As it is an invisible, odorless, and flammable gas, it is necessary to detect hydrogen leakage in the environment. There is a strong need to develop novel hydrogen sensors for: solid oxide fuel cells [2,3], hydrogen engine cars [1,4], transportation and storage of H<sub>2</sub> [5] or other applications. Nowadays, H<sub>2</sub> is used as the fuel for the internal combustion engines and fuel cells that may soon flood into the automotive industry and customers houses due to the potential for substantially cleaner emissions than internal combustion engines. Thus, to control the energy conversion processes in such engines and fuel cells it will require numerous hydrogen sensors for each unit. It is evident that the cost, compactness, reliability and selectivity along with technical requirements on such devices are major specifications which have to be considered when sensors were developed. Also, the importance of development of a nanosensor with ability to selectively detect hydrogen at room temperature

\* Corresponding author. Address: Department of Physics, University of Central Florida, 4000 Central Florida Boulevard, Orlando, FL 32816-2385, USA. Tel.: +1 407 823 2333; fax: +1 407 823 5112.

E-mail address: [lupan@physics.ucf.edu](mailto:lupan@physics.ucf.edu) (O. Lupan).

is driven by the fact that, in most of the field applications, hydrogen is to be detected at the presence of other combustible gases, such as hydrocarbons and volatile organic compounds [6], with presence of air in the ambient. Recently the main effort of H<sub>2</sub> sensor development has been the improvement of H<sub>2</sub> gas sensitivity as well as selectivity and to decrease the operating temperature. A compact, reliable, inexpensive, and low power consumption sensor device that can detect hydrogen have been subject of many research groups [2–11].

ZnO is one of the most promising and useful materials for gas sensors, especially for H<sub>2</sub> sensing [2–12]. However the sensitivity of the ZnO bulk material is not sufficiently high. Nano-ZnO possesses large surface area, thermal and mechanical stability [13], and radiation hardness [14] and is compatible with other nanodevices. The physical properties of the nano-ZnO depend on the microstructure of the materials, including crystal size, morphology, orientation, aspect ratio and crystalline density [15]. Sensing properties of ZnO are directly related to its preparation history, particle size, morphology and operating temperature. The sensor signal consists of relative resistance changes due to gas adsorption on the surface of nano-ZnO and permits real-time detection. Thus, bio-safe and biocompatible ZnO nanoarchitectures are most attractive candidates for this type of sensing and requirements, and are intensively investigated nowadays.

Several nano-ZnO-based H<sub>2</sub> sensors have been reported. For example pure and Pd-coated multiple ZnO nanorods [2,16], Pt-coated ZnO thin films and nanorods [3], ZnO nanorod arrays [2], multiple ZnO nanorods [8], single nanowires of metal oxides [17], metallic catalyst coatings (Pd, Pt, Au, Ag, Ti and Ni) on multiple ZnO nanorods [18]. However, for production purpose, an inexpensive and bio-safe synthesis process is required [19–21]. It has been pointed out that there are disadvantages of nanorods/nanowires currently used in sensors [22], including increased complexity, lengthy sample preparation, device fabrication, time consuming analysis, or lack of selectivity. At the same time, the features of the nanowire synthesis method desired for industry are low-cost materials and processing, control of process parameters, environment friendly reagents, etc. [21]. To overcome some of these limitations and to bridging between the laboratory and industry, we have focused on nanofabrication of transferable single ZnO nanorod as the building block for a high selectivity H<sub>2</sub> sensor that can be operated at room temperature. Uses of catalyst or growth seed layer for the nanorod grows were not needed in our novel nanofabrication technique.

In this paper we report the fabrication of single ZnO nanorod based hydrogen sensor using focused ion beam in-situ lift-out technique. Fabricated nanosensor is capable of detection of 100–200 ppm hydrogen in air at room temperature.

## 2. Experimental details

### 2.1. Synthesis and characterizations

ZnO nanorods have been grown using a bio-safe hydrothermal method. Starting materials are analytical grade zinc sulfate (Zn(SO<sub>4</sub>) · 7H<sub>2</sub>O) and ammonia solution (NH<sub>4</sub>OH) from Fisher Scientific. Zn(SO<sub>4</sub>) · 7H<sub>2</sub>O (0.10–0.15 M) and NH<sub>4</sub>OH (29.6%) were mixed with 50 ml de-ionized (DI) water (~18 MΩ cm). In this process – glass, quartz or Si substrates were first cleaned using procedures described in Ref. [23]. This cleaning procedure permits a uniformly wettable substrate surface. Afterward the substrates were placed directly in an aqueous complex solution reactor as described in Ref. [23]. It was mounted on a pre-heated laboratory oven and kept at 75–95 °C for 10 min. After that the substrates were washed with DI water and finally, the product was dried in air at 150 °C for 10 min. Rapid thermal processing of grown ZnO nanoarchitectures at 600 °C for a duration of 60 s was realized, according to previous reports [23–25]. Rapid thermal annealing in 30–60 s after synthesis of ZnO nanorods determine desorption of the large number of chemisorbed oxygen species at the surface of freshly prepared zinc oxide samples. The loss of adsorbed oxygen increases the electron concentration of the surface and improves the conductance.

### 2.2. Characterization techniques

Crystal structure identification of ZnO nanorods was obtained using a Rigaku 'D/B max' X-ray diffractometer with a CuKα radiation ( $\lambda = 1.54178 \text{ \AA}$ ) at a scanning rate of 0.04°/s in the  $2\theta$  range from 10° to 90°. Morphology of the nanostructures was identified by a scanning electron microscope (SEM) Hitachi S800. The sizes and crystal structure of the nanorods were recorded with a FEI Tecnai F30 transmission electron microscope (TEM) using accelerating voltage 300 kV. The composition of ZnO was characterized by energy dispersive X-ray spectrometer (EDX). These investigations confirmed that these nanorods are crystalline and regular distributed throughout the substrate surface.

The hydrogen gas sensing characteristics were investigated using a single ZnO nanorod, with a measuring apparatus consisting of a closed quartz chamber connected to a gas flow system. The

concentration of test gases was measured using pre-calibrated mass flow controller. Hydrogen and air were introduced to a gas mixer via a two-way valve using separate mass flow controllers. The test gases were allowed to flow through a pipe network of diameter of 5 mm to a test chamber. The mixed gas was injected to a test chamber with a sensor holder, in which the nanosensor was placed. The gas flow was maintained by using mass flow controllers. By monitoring the output voltage across the nanorod based sensor, the resistance was measured in dry air and in a test gas. A computer with suitable lab-view interface handled all controls and acquisition of data.

## 3. Results and discussion

### 3.1. Crystal structure and morphology analysis of the nanorods

Fig. 1 depicts typical XRD spectrum of ZnO nanorods grown in 10 min at 90 °C by aqueous solution technique. All the diffraction peaks in the pattern are indexed as the hexagonal wurtzite ZnO structure with lattice constants in accordance with values in the standard card (space group: P<sub>6</sub>mc(186);  $a = b = 0.3249 \text{ nm}$ ,  $c = 0.5206 \text{ nm}$  and the data are in agreement with JCPDS card number 36-1451 for ZnO) [26]. No other minority phase peaks were detected.

The quality of the grown ZnO rods was also confirmed by the 1.0:1.0 stoichiometric composition deduced from the EDX analysis.

X-ray photoelectron spectroscopy (XPS), TEM and micro-Raman characterization results has been discussed in details in our previous work [23].

Comparatively to other synthetic methods of ZnO, the developed aqueous solution chemical deposition process used in our research make possible the production of large quantities of transferable nanorods in a reproducible way. Distinct advantages of our technique are: (a) growth at relatively low temperature (75–95 °C), (b) short growth interval of 10–20 min, and (c) products are transferable to other substrates.

In our experimental conditions, a novel one-dimensional (1D) nanostructure of ZnO nanorods with perfect hexagonal cross-section as building blocks for nanodevices are synthesized. A typical scanning electron micrograph (SEM) of as-grown transferable ZnO nanorods are shown in Fig. 2, insert shows ZnO nanorod arrays grown on substrate simultaneously.

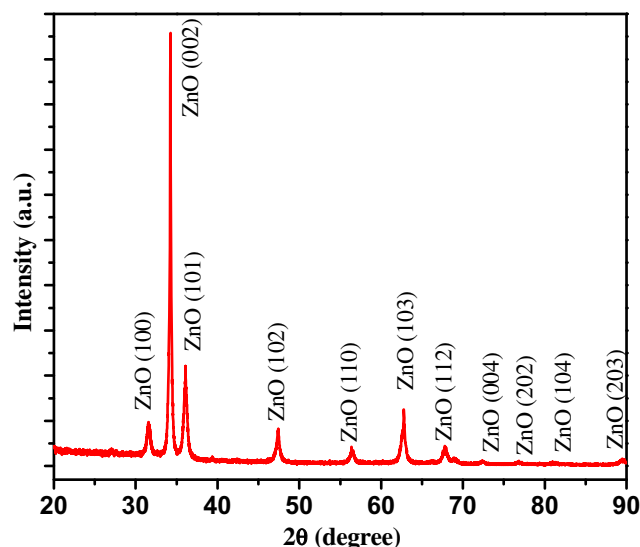
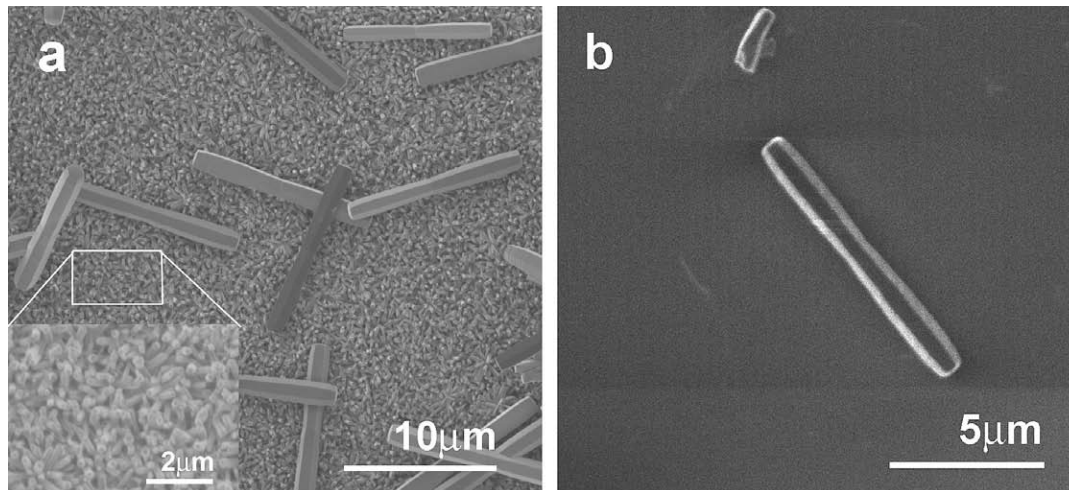


Fig. 1. XRD pattern of the ZnO nanorods synthesized by aqueous-solution method at 90 °C for 10 min in the solution.



**Fig. 2.** Scanning electron micrographs of ZnO nanorods: (a) as-grown on initial glass substrate; inset shows nanorod arrays grown on substrate and (b) transferred to Si/SiO<sub>2</sub> substrate, and distributed on the surface in order to be picked-up by the in-situ lift-out needle in the focused ion beam FIB/SEM system.

For the sensor fabrication, the Si/SiO<sub>2</sub> wafers were used as intermediate substrate for nanorods transferring and individual distribution for an easy further pick-up by in-situ lift-out technique.

In Fig. 2b we showed the single ZnO rod that were transferred to a Si/SiO<sub>2</sub> substrate. We can see that in the transfer process, we reduced the density of nanorods on the surface of the substrate and the substrate surface is much cleaner. This will facilitate the in-situ FIB/SEM process of the nanorod devices fabrication.

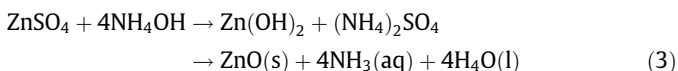
The growth mechanism of ZnO one-dimensional nanorods in aqueous solution of zinc sulfate and ammonia can be explained by considering that ZnO wurtzite crystals have different growth rates for different planes:  $V_{<001>} > V_{<101>} > V_{<100>}$ . Thus, the faster the growth rate, the quicker the disappearance of the plane perpendicular to the growth direction and leads to respective shape in an end of the axis. These will result in one-dimensional ZnO nanorods with a perfect hexagonal cross-section, as can be seen from Fig. 2a. The nanorod crystal synthesis on a specific surface in the aqueous solution is based on heterogeneous nucleation and subsequent growth under kinetic growth conditions.

Ammonia, which was used in the synthesis of ZnO nanorods, provides the hydroxide ions (OH<sup>-</sup>) and also ammonia molecules (NH<sub>3</sub>) in the aqueous solution. Thus two complexes [Zn(OH)<sub>4</sub>]<sup>2-</sup> and tetraaminezinc(II) [Zn(NH<sub>3</sub>)<sub>4</sub>]<sup>2+</sup> were formed in reactor with complex solution used for ZnO nanorods growth. It has been shown that the ratio of Zn(OH)<sub>2</sub> to tetraaminezinc(II) [Zn(NH<sub>3</sub>)<sub>4</sub>]<sup>2+</sup> determines the morphology of ZnO nanocrystals [27]. Formation of two complexes can be described as follow:



Thus, two reactions can take place under described conditions in the aqueous solution, resulting in the formation of ZnO.

One route for ZnO crystal growth by aqueous solution deposition can be described as follows:



The growth of ZnO nanorods in aqueous solution takes place when the temperature increases. When the concentration of Zn<sup>2+</sup> and OH<sup>-</sup> exceed supersaturation, ZnO nuclei are formed at the interface between substrate and solution. After that, the crystals will grow into nanorod arrays as is represented in Fig. 2a (insert). The [Zn(OH)<sub>4</sub>]<sup>2-</sup> ions decompose to produce ZnO molecular species

[28] which form seeds and grow to form hexagonal nucleus and finally nanorod arrays on the substrate as background (see insert in Fig. 2a). The reaction steps can be described as following: first is the formation of complex [Zn(OH)<sub>4</sub>]<sup>2-</sup> according to Eq. (1), then deprotonation of the hydrated zinc species to form oxide

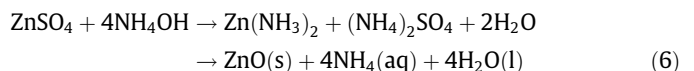


this reaction will form ZnO on substrate and will leave 2OH<sup>-</sup> in solution. Due to the stability of the second complex, tetraaminezinc(II) is higher than that of the [Zn(OH)<sub>4</sub>]<sup>2-</sup>, [Zn(NH<sub>3</sub>)<sub>4</sub>]<sup>2+</sup> formed as a result of Eq. (2) will react with 2OH<sup>-</sup> (the equilibrium moves to the right at temperatures >75 °C [29]). The interface between the substrate and the solution provided the nucleation sites for the growth of ZnO nuclei:



On the surface of ZnO nuclei were absorbed OH<sup>-</sup> with negative charge and the remaining tetraaminezinc(II) complexes will deposited according to Eq. (5).

Another route for ZnO nanorods growth by aqueous solution deposition is



Transferable ZnO nanorods grew directly in solution, rather than the substrate after hetero-nucleation with a lower activation energy barrier. It should be pointed out, that it is necessary to control carefully heterogeneous nucleation due to random and complex nature of nucleation. Therefore, pre-coated substrate in the first reaction Eq.(3) (which take place simultaneously with the second one Eq. (6)) with nanorod arrays of the same material is an excellent way to control the morphology and orientation of desired transferable nanorods. By controlling the degree of supersaturation and keeping the reaction temperature low, massive precipitation can be avoided. NH<sub>3</sub> and Zn(NH<sub>3</sub>)<sub>4</sub><sup>2+</sup> cause the ZnO crystal to grow in the *c*-direction according to previous reports [30].

The reason ZnO nanorods can grow in 10–15 min can be explained by higher-symmetry (C<sub>6v</sub>) for polar plane <001> than those along other directions [31]. Thus, the controlled synthesis of 1D nanoarchitectures can be realized by altering Zn<sup>2+</sup>/OH<sup>-</sup> ratio.

In the case for Zn<sup>2+</sup>/OH<sup>-</sup> ratio of 1:2, wurtzite ZnO crystal zinc terminated (001) planes, are terminated with Zn ions which are active and promote 1D growth [32,33]. One face of the hexagonal

sheet is Zn rich and forms (001) planes, while the opposite face is the (00 $\bar{1}$ ) plane. The ZnO nanocrystals are polar in nature, and the Zn-rich positive (001) surface is more reactive than the oxygen-rich negative (00 $\bar{1}$ ) surface and attracting new ZnO species to the surface and promoting anisotropic growth along the (001) direction [32].

Based on the “lowest-energy” theory [33] that dictates the preferred growing direction, the growth mechanism also can be explained. Our technique is energetically more preferential (e.g. influence of seeding on nanorods growth) because it takes place at relative low temperature (75–95 °C) in short time (10–15 min).

According to our experimental results, the nanorods obtained by our process can be easily transferred to other Si/SiO<sub>2</sub> substrates and distributed on the surface (Fig. 2b) of other substrates for further processing by the in-situ lift-out processes.

### 3.2. Nanofabrication of sensors by in-situ lift-out technique

Next the in-situ lift-out procedure is described. Usually a microscope and a micromanipulator for the ex-situ lift-out technique has been used to separate individual ZnO nanorods in order to be easily attached to the in-situ FIB needle. A 100 $\times$  magnification was used to locate ZnO nanorods on the intermediate Si/SiO<sub>2</sub> substrate in order to avoid charging problems in the FIB system. A magnification of 7000 $\times$  was used to lift the single ZnO nanorod.

A Keindiek Micromanipulator used in our work permits movements of a few nanometers along the *x* and *y* directions and 1 nm movements in the *z* direction. Micromanipulator was mounted next to the stage. Sample on the stage can be rotated, tilted perpendicular to either beam which enable easy arrangement of single ZnO nanorod on the nanosensor template. For the nanosensor preparation, the glass substrate was used and Al electrodes were deposited as template with external electrodes/connections. The needles used for the lift-out step were electro-polished tungsten wire.

The next step in our procedure is to scan the surface of the intermediate Si/SiO<sub>2</sub> substrate for convenient placed intermediate

ZnO nanorod. Then the needle was lowered and bringing into the FIB focus and its tip positioned at the close end of the intermediate nanorod as shown in Fig. 3a. Before attaching of selected nanorod it is recommended to push it with FIB needle in order to make sure that it is not attached firmly to the substrate. In the in-situ lift-out process [7,34], we found that attachment of single intermediate nanorod on the top of the FIB needle (Fig. 3a and b) will permit an easy pick-up of the selected nanorod to be further handled. This intermediary step makes it possible to fabricate nanodevice much faster.

During this step, the needle was lowered and its tip positioned at one end of an intermediate nanorod as shown in Fig. 3a. The needle was then moved until touched the nanorod. Then the nanorod was attached to the end of the FIB needle as shown in Fig. 3b by deposition of 0.5  $\mu$ m Pt film.

The next step was to scan the Si/SiO<sub>2</sub> substrate for well-placed ZnO nanorod. Once a desired nanorod was identified the previous attachment procedure was repeated (Fig. 3c). Following this step the needle and specimen was raised away from the substrate.

Fig. 3d shows a square hole fabricated on the glass substrate area in order to allow entire surface of ZnO nanorod to be involved in the H<sub>2</sub> sensing process. Inset in Fig. 3c shows nanosensor substrate template (glass with Al contacts as contact electrodes). Using micromanipulator, we carefully positioned ZnO nanorod over the square hole (Fig. 3e). In the last step, the ZnO nanorod was fixed to one of the pre-deposited electrodes/external contacts. The nanorod is cut and the needle raised away from the substrate. Fig. 3f shows the fabricated single nanorod-based nanosensor. The typical time to perform this in-situ lift-out FIB nanofabrication is about 20–35 min. Also taken in the account that nanorod synthesis was done in 10 min, we substantially contribute to overcome some obstacles and conception that nanorods/nanowires are not convenient [20] for sensor production. Our success rate using this described steps is >90%. This minimizes FIB processing time for the experimental nanodevice fabrication and can be extended for other nanodevices. The typical time taken to perform this in-situ lift-out FIB nanofabrication is 20–35 min. At the same time we satisfied the

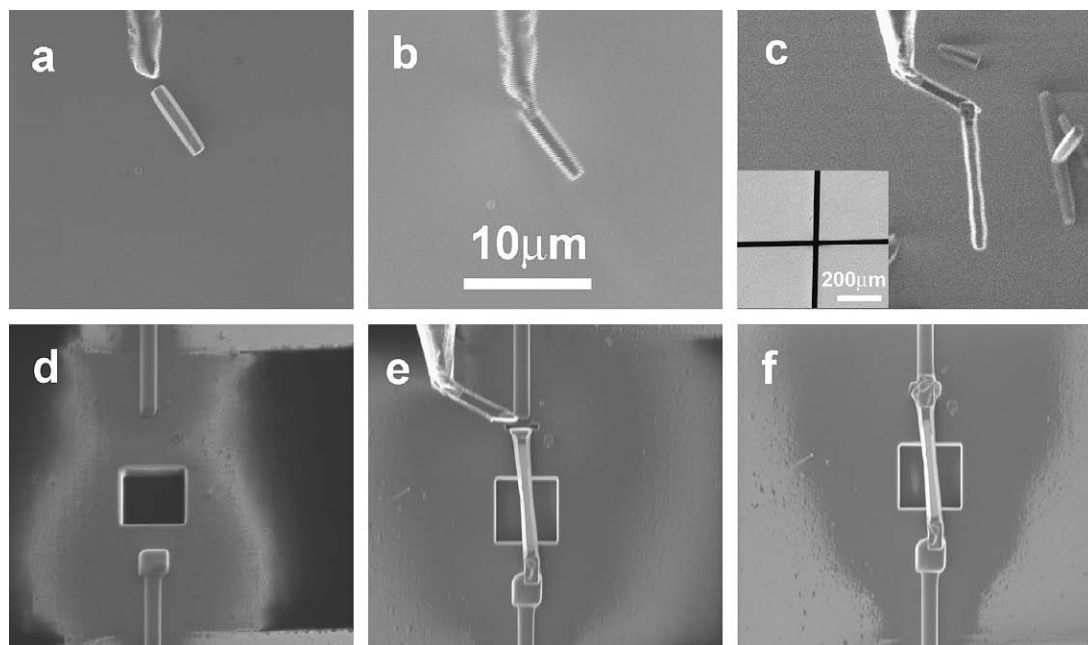


**Fig. 3.** Scanning electron SEM images showing the steps of the in-situ lift-out fabrication procedure in the FIB/SEM system. (a) an intermediate ZnO nanorod on Si substrate, next to the FIB needle; (b) an intermediate ZnO nanorod – picked-up by the needle; (c) a single ZnO nanorod selected for sensor fabrication. Inset shows nanosensor substrate template (glass with Al contacts as contact electrodes); (d) a square hole cut on the glass; (e) place the ZnO nanorod over the hole; (f) single nanorod welded to both electrode/external connections as final sensor.

features of the nanowire synthesis method desired for industry are low-cost materials and processings, control of process parameters, environment friendly reagents, etc [20]. The main advantage of this procedure is a quick verification/testing of concept and the procedure is compatible with micro/nanoelectronic devices.

### 3.3. Gas sensing properties

The fabricated single ZnO nanorod-based nanosensor was put in a test chamber to detect H<sub>2</sub> and other gases, such as O<sub>2</sub>, CH<sub>4</sub>, CO, ethanol and LPG. It was found that resistance change  $|\Delta R| = |R_{\text{air}} - R_{\text{gas}}|$  increased linearly with H<sub>2</sub> gas concentration, where  $R_{\text{air}}$  the resistance of the sensor in dry air and  $R_{\text{gas}}$  is resistance in the test gas. The gas sensitivity (response value) of the nanosensor was obtained using relationship:

$$S = \frac{|\Delta R|}{R} \quad (7)$$

After the exposure to hydrogen sensor were maintained for a recovering period in dry air. The room temperature sensitivity of the single nanorod ZnO nanosensor to 200 ppm H<sub>2</sub> is shown in Fig. 4. Response time constants are on the order of 30 s and after 40 s the signal reach the equilibrium value after the H<sub>2</sub> test gas was injected. The relative resistance changes were about 4%. The resistance was restored toward the 10% above the original value within 50–90 s of introducing clean air. This suggests a reasonable recovery time. The sensor showed relatively fast response and baseline recovery for 200 ppm H<sub>2</sub> detection at room temperature.

Several ZnO nanorod hydrogen sensors have been reported in the literature. The multiple pure ZnO nanorod-based sensor presented in [2] has a sensitivity of ~0.25% at 500 ppm H<sub>2</sub> in N<sub>2</sub> after 10 min exposure. However, the Pd-coated ZnO nanowires gas sensors, showed a higher H<sub>2</sub> sensitivity (4.2%) and fast response/recovery time at concentration up to 500 ppm at the room temperature [2]. Furthermore sensor based on ZnO multiple nanorods and exposed under 10% H<sub>2</sub> in N<sub>2</sub> at 112 °C, showed high sensitivity ~18% of current change [12].

By comparison, our single ZnO nanorod sensor exposed to 200 ppm H<sub>2</sub> shows a relative response ~4% in 30–40 s, while Rout et al. [17] showed that single ZnO nanowires have a sensitivity of ~300% for 100 ppm H<sub>2</sub> at room temperature. The sensitivity  $\Delta R/R \sim 4\%$  of our sensor is attractive for further investigation of single ZnO nanorod for practical H<sub>2</sub> sensor applications.

These experimental results ensure application of our novel sensors to detect H<sub>2</sub> at low ppm range (1–1000 ppm) at room temper-

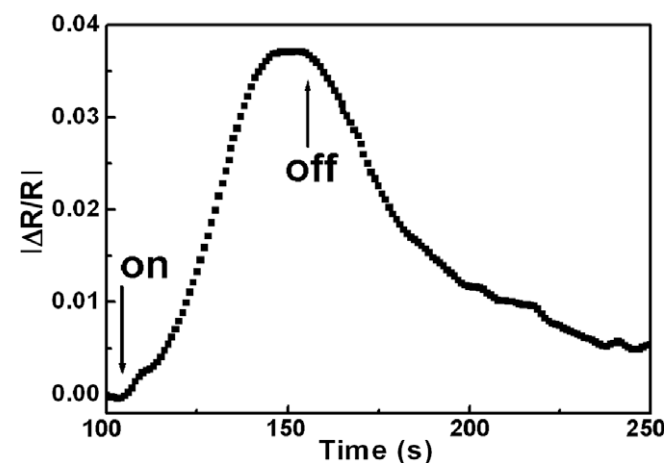


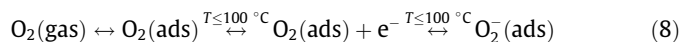
Fig. 4. The room temperature relative response of the conductometric single ZnO nanorod-based H<sub>2</sub> nanosensor fabricated by in-situ lift-out technique in the FIB system.

ature. According to Fig. 3d where it is shown a square hole fabricated on the glass substrate area in order to allow entire surface of nanorod to be involved in the H<sub>2</sub> sensing process. Using such construction/structure of the fabricated nanosensor was increased sensitivity twice comparing with the investigated sensors without a square hole fabricated under it. We found that our single ZnO nanorod sensor has a gas sensitivity of less than 0.25% for O<sub>2</sub>, CH<sub>4</sub>, CO, ethanol and LPG under the same conditions. Fig. 5 shows sensitivity to different gases.

The adsorption–desorption sensing mechanism can be explained on the base of reversible chemisorption of the hydrogen on the ZnO nanorod. It produces a reversible change in the resistivity with the exchange of charges between H<sub>2</sub> and the ZnO surface leading to changes in the depletion length [35,36]. One of the intuitive effects in sensitivity improvement is due to the change in the surface/volume ratio [37].

It is well known that oxygen is adsorbed on a ZnO nanorod surface as O<sub>2</sub><sup>-</sup>, O<sup>-</sup>, and O<sup>2-</sup> ions by extracting electrons [38,39] from the conduction band. Sensing mechanism is based on interaction between the negatively charged oxygen adsorbed on the zinc oxide surface and hydrogen gas to be detected.

Initially the molecular oxygen are adsorbed on the surface of ZnO nanorod and electrons are consumed following the reactions:



thus increase of the nanorod resistance.

When the ZnO nanorod sensor is exposed to a reducing test gas such as hydrogen, its atoms react with these chemisorbed oxygen ions and produce H<sub>2</sub>O molecules consuming chemisorbed oxygen from the nanorod surface by releasing electrons. The sensing mechanism for H<sub>2</sub> at room temperature can be represented by the following relation:



considering O<sub>2(ads)</sub><sup>-</sup> as the predominant adsorbed species on ZnO nanorod surface at room temperature [36]. As a result electrons will be released back to the conduction band and will contribute to current increase through the nanorod. This also results in a reduction of surface depletion region and increase conductivity. The reaction is exothermic in nature (1.8 kcal mol<sup>-1</sup>) [39] and the molecular water desorbs quickly from the surface. Due to the fact that water forming reaction is sophisticated and mechanism is not well defined, therefore the H<sub>2</sub> sensing mechanism still needs more understanding.

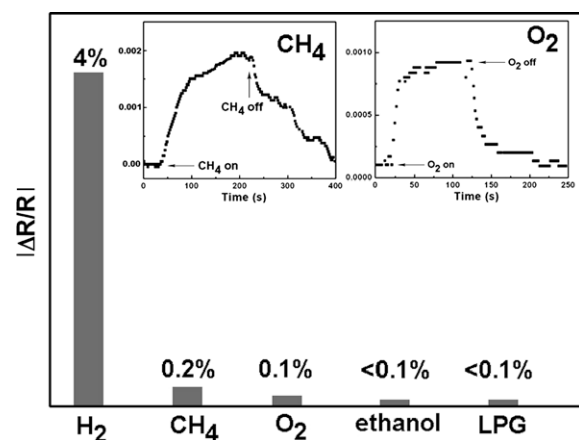


Fig. 5. The room temperature relative response of the single ZnO nanorod-sensor to different gases. Insert is relative response to CH<sub>4</sub> and O<sub>2</sub> at room temperature of single rod-sensor.

#### 4. Conclusion

In summary, to our knowledge, this work demonstrates, for the first time, single ZnO nanorod hydrogen sensor synthesized through a low-temperature aqueous solution route. The major advantages of this method are its simplicity and fast growth rates (10 min versus several hours). We also showed that the morphology and distribution of nanorods can be effectively controlled by using suitable preparing conditions. The ZnO nanorods growth mechanism based on the ratio of  $\text{Zn}(\text{OH})_2$  to tetraaminezinc(II)  $[\text{Zn}(\text{NH}_3)_4]^{2+}$  is proposed to explain the formation of ZnO nanorod arrays and transferable nanorods.

In addition, an in-situ lift-out technique has been presented to fabricate single ZnO nanorod  $\text{H}_2$  sensor. The main advantage of the proposed synthesis is its simplicity and fast growth method. The typical time taken to perform this in-situ lift-out FIB/SEM nanofabrication is 20–35 min. Also taken in the account that nanorod synthesis takes about 10 min, we contribute to overcome some obstacles for nanorods/nanowires sensor production. The ~4% sensitivity to  $\text{H}_2$ , quick response and recovery times, and selectivity were found to be significant useful for further development of  $\text{H}_2$  nanosensor at room temperature. It is anticipated that techniques described in this work offers solutions to controlling nanorods growth and to fabricate nanodevices on it.

#### 4.1. Further work

Our further research efforts are directed towards synthesizing oriented one-dimensional nanorods, which will facilitate construction of semiconductor nanodevices with well-ordered alignment, which are extremely important for scientific, technological and industrial application. Development of single doped ZnO nanorod sensor for biosensing. Also *p-n* junction in a transferable single nanorod can promote next generation of nanodevices.

#### Acknowledgments

The research described in this publication was made possible in part by Award No. MTFP-1014B Follow-on Award (for young researchers) of the Moldovan Research and Development Association (MRDA) and the US Civilian Research and Development Foundation (CRDF). Dr. L. Chow acknowledges partial financial support from Apollo Technologies Inc. and Florida High Tech Corridor research program.

#### References

- [1] Basic Research Needs to Assure a Secure Energy Future, A Report from the Basic Energy Sciences Advisory Committee, February 2003, available

- from: <[http://www.sc.doe.gov/bes/besac/Basic\\_Research\\_Needs\\_To\\_Assure\\_A\\_Secure\\_Energy\\_Future\\_FEB2003.pdf](http://www.sc.doe.gov/bes/besac/Basic_Research_Needs_To_Assure_A_Secure_Energy_Future_FEB2003.pdf)>.
- [2] H.T. Wang, B.S. Kang, F. Ren, L.C. Tien, P.W. Sadik, D.P. Norton, S.J. Pearton, J. Appl. Phys. Lett. 86 (2005) 243503.
- [3] L.C. Tien, P.W. Sadik, D.P. Norton, L.F. Voss, S.J. Pearton, H.T. Wang, B.S. Kang, F. Ren, J. Jun, J. Lin, Appl. Phys. Lett. 87 (2005) 222106.
- [4] S. Verhelst, R. Sierens, Int. J. Hydrogen Energy 26 (2001) 987–990.
- [5] X. Bevenot, A. Trouillet, C. Veillas, H. Gagnaire, M. Clement, Sens. Actuators B Chem. 67 (2000) 57–67.
- [6] Y.-D. Wang, C.-L. Ma, X.-H. Wu, X.-A. Sun, H.-D. Li, Sens. Actuators B Chem. 85 (2002) 270–276.
- [7] O. Lupan, G. Chai, L. Chow, In-situ lift-out fabrication and characterizations of ZnO branched nanorods-based sensors, in: NSTI Nanotechnology Conference and Trade Show, Santa Clara, California, USA, May 20–24, 2007.
- [8] C.S. Rout, A.R. Raju, A. Govindaraj, C.N.R. Rao, Solid State Commun. 138 (3) (2006) 136.
- [9] J.R. LaRoche, Y.W. Heo, B.S. Kang, L.C. Tien, Y. Kwon, D.P. Norton, B.P. Gila, F. Ren, S.J. Pearton, J. Electron. Mater. 34 (4) (2005) 404.
- [10] J.X. Wang, X.W. Sun, Y. Yang, H. Huang, Y.C. Lee, O.K. Tan, L. Vayssieres, Nanotechnology 17 (19) (2006) 4995.
- [11] L. Liao, H.B. Lu, J.C. Li, H. He, D.F. Wang, D.J. Fu, C. Liu, W.F. Zhang, J. Phys. Chem. C 111 (5) (2007) 1900.
- [12] B.S. Kang, Y.W. Heo, L.C. Tien, D.P. Norton, F. Ren, B.P. Gila, S.J. Pearton, Appl. Phys. A 80 (2005) 1029.
- [13] I. Yonenaga, Phys. B: Condens. Matter 308–310 (2001) 1150.
- [14] D.C. Look, Mater. Sci. Eng. B 80 (2001) 383.
- [15] Z.R. Tian, J.A. Voigt, J. Liu, B. McKenzie, M.J. Mcdermott, M.A. Rodriguez, H. Konishi, H. Xu, Nature Mater. 2 (12) (2003) 821.
- [16] L.C. Tien, H.T. Wang, B.S. Kang, F. Ren, P.W. Sadik, D.P. Norton, S.J. Pearton, J. Lin, Electrochem. Solid-State Lett. 8 (9) (2005) G230.
- [17] C.S. Rout, G.U. Kulkarni, C.N.R. Rao, J. Phys. D: Appl. Phys. 40 (2007) 2777.
- [18] H.T. Wang, B.S. Kang, F. Ren, L.C. Tien, P.W. Sadik, D.P. Norton, S.J. Pearton, J. Lin, Appl. Phys. A: Mater. Sci. Proc. 81 (6) (2005) 1117.
- [19] E. Galoppini, J. Rochford, H. Chen, G. Saraf, Y. Lu, A. Hagfeldt, G. Boschloo, J. Phys. Chem. B 110 (2006) 16159.
- [20] A. Du Pasquier, H. Chen, Y. Lu, Appl. Phys. Lett. 89 (2006) 253513.
- [21] K.S. Shankar, A.K. Raychaudhuri, Mater. Sci. Eng. C 25 (2005) 738–751.
- [22] C. Wang, X. Chu, M. Wu, Sens. Actuators B Chem. 113 (1) (2006) 320.
- [23] O. Lupan, L. Chow, G. Chai, B. Roldan, A. Naitabdi, A. Schulte, Mater. Sci. Eng. B: Solid-State Mater. Adv. Technol. 145 (2007) 57–66.
- [24] O.I. Lupan, S. Shishiyanu, L. Chow, T. Shishiyanu, Thin Solid Films 516 (10) (2008) 3338–3345.
- [25] S.T. Shishiyanu, O.I. Lupan, E.V. Monaico, V.V. Ursaki, T.S. Shishiyanu, I.M. Tiginyanu, Thin Solid Films 488 (2005) 15.
- [26] Joint Committee on Powder Diffraction Standards, Powder Diffraction File No. 36-1451.
- [27] H. Zhang, D. Yang, D.S. Li, X.Y. Ma, S.Z. Li, D.L. Que, J. Cryst. Growth Des. 5 (2005) 547.
- [28] A. Dev, S. Kar, S. Chakrabarty, S. Chaudhuri, Nanotechnology 17 (2006) 1533.
- [29] Z. Wang, X.F. Qian, J. Yin, Z.K. Zhu, Langmuir 20 (2004) 3441.
- [30] J. Zhang, L.D. Sun, J.L. Yin, H.L. Su, C.S. Liao, C.H. Yan, Chem. Mater. 14 (2002) 4172.
- [31] C.X. Xu, X.W. Sun, Jpn. J. Appl. Phys. 42 (2003) 4949.
- [32] S. Kar, A. Dev, S. Chakrabarty, S. Chaudhuri, J. Phys. Chem. B 110 (2006) 17848.
- [33] L. Guo, Y. Ji, Am. Chem. Soc. 124 (2002) 14864.
- [34] O. Lupan, G. Chaj, L. Chow, Microelectron. J. 38 (2007) 1211.
- [35] H.L. Hartnagel, A.L. Dawar, A.K. Jain, C. Jagadish, Semiconducting Transparent Thin Films, IOP, Bristol, 1995.
- [36] G. Heiland, D. Kohl, in: T. Seiyama (Ed.), Chemical Sensor Technology, 1, Kodansha, Tokyo, 1983, p. 113.
- [37] J. Riu, A. Maroto, F.X. Rius, Talanta 69 (2) (2006) 288.
- [38] A.R. Raju, C.N.R. Rao, Sens. Actuators B Chem. 3 (4) (1991) 305.
- [39] S. Saito, M. Miyayama, K. Kuomoto, H. Yanagida, J. Am. Ceram. Soc. 68 (1985) 40.